An open-source platform for 3D transcranial Ultrasound Localization Microscopy in awake mice

Georges Chabouh, Louise Denis, Myriam Abioui-Mourgues, Jean-Baptiste Deloges, Jacques Battaglia, Arthur Chavignon, Baptiste Heiles, Basile Pradier, Sylvain Bodard, Denis Vivien, et al.

An open-source platform for 3D transcranial Ultrasound Localization Microscopy in awake mice

Georges Chabouh

georges.chabouh@sorbonne-universite.fr

Laboratory for biomedical Imaging Sorbonne University CNRS INSERM https://orcid.org/0000-0003-0760-909X

Louise Denis

Laboratory for biomedical Imaging Sorbonne University CNRS INSERM

Myriam Abioui-Mourgues

UNICAEN, Caen Normandie Universit ´ e,Inserm UMR-S U1237, Physiopathology and Imaging of Neurological Disorders (PhIND), GIP Cyceron, Institut Blood and Brain @ Caen-Normandie (BB@C)

Jean-Baptiste Deloges

Laboratory for biomedical Imaging Sorbonne University CNRS INSERM https://orcid.org/0000-0001-5753-1994

Jacques Battaglia

Laboratory for biomedical Imaging Sorbonne University CNRS INSERM

Arthur Chavignon

Laboratoire d'Imagerie Biomédicale https://orcid.org/0000-0001-7883-7482

Baptiste Heiles

Department of Imaging Physics, TU Delft, Netherlands https://orcid.org/0000-0001-9254-1741

Basile Pradier

Laboratory for biomedical Imaging Sorbonne University CNRS INSERM

Sylvain Bodard

AP-HP, Hopital Necker Enfants Malades, Service d'Imagerie Adulte, Paris, France Laboratory for biomedical Imaging Sorbonne University CNRS INSERM

Denis Vivien

Normandie Univ, UNICAEN, INSERM, U1237, PhIND "Physiopathology and Imaging of Neurological Disorders", Institut Blood and Brain @ Caen-Normandie, Cyceron https://orcid.org/0000-0002-7636-2185

Cyrille Orset

UNICAEN, Caen Normandie Universit ´ e,Inserm UMR-S U1237, Physiopathology and Imaging of Neurological Disorders (PhIND) GIP Cyceron, Institut Blood and Brain @ Caen-Normandie (BB@C)

Olivier Couture

Laboratoire d'Imagerie Biomédicale, Sorbonne Université, CNRS, INSERM https://orcid.org/0000-0002-8683-1424

Article

Keywords:

Posted Date: September 9th, 2024

DOI: https://doi.org/10.21203/rs.3.rs-4925712/v1

Additional Declarations: Yes there is potential Competing Interest. Olivier Couture is the holder of patents concerning super-resolution ultrasound imaging. He is also a co-founder and share-holder in the startup ResolveStroke.

An open-source platform for 3D transcranial Ultrasound Localization Microscopy in awake mice

Georges Chabouh[1,#,*], Louise Denis[1,#], Myriam Abioui-Mourgues[2], Jean-Baptiste Deloges[1], Jacques Battaglia[1], Arthur Chavignon[1], Baptiste Heiles[3], Basile Pradier[1], Sylvain Bodard[1,5], Denis Vivien[2,4], Cyrille Orset[2], and Olivier Couture[1,*]

[1] Sorbonne Université, UMR 7371 CNRS, Inserm U1146, Laboratoire d'Imagerie Biomedicale, 15 Rue de l'Ecole de Médecine, 75006 Paris, France
[2] UNICAEN, Caen Normandie Université,Inserm UMR-S U1237, Physiopathology and Imaging of Neurological Disorders (PhIND), GIP Cyceron, Institut Blood and Brain @ Caen-Normandie (BB@C), Normandie University, Caen, France
[3] Division of Chemistry and Chemical Engineering, California Institute of Technology, Pasadena, CA, USA
[4] Department of Clinical Research, Caen-Normandie University Hospital, CHU Caen, Avenue de la Côte de Nacre, Caen, France
[5] AP-HP, Hôpital Necker Enfants Malades, Service d'Imagerie Adulte, Paris, France
[#] These authors have contributed equally
[*] georges.chabouh@sorbonne-universite.fr, olivier.couture@sorbonne-universite.fr

ABSTRACT

We present an open-source code for 3D super-resolution ultrasound imaging. Open-3DULM was applied to transcranial imaging in habituated awake mice. Comparative analysis reveals that isoflurane anesthesia induces significant vasodilation and higher cerebral blood flow compared to the awake state. This method could serve as a reference for developing new types of 3D vascular quantifications, particularly emphasizing the importance of awake and 3D imaging for accurate cerebral blood flow measurement in neuroscience research.

Ultrasound localization microscopy (ULM) is the leading technique for super-resolution ultrasound imaging[1–5] because it excels in visualizing capillary-scale vessels within a variety of organs, including the human brain[6], heart[7], and kidneys[8–10]. ULM is mostly implemented in 2D which represents various limitations such as user dependency, out of plane motion and imprecise quantification[11]. Volumetric ULM, or 3D ULM[12–14], allows appropriate quantification of microbubbles[15] and tissue motion, along with organ-wide acquisitions within the time of a single contrast agent's bolus (minutes).

To prevent pain, stress, and motion artifacts in animal imaging, animals are routinely scanned with various imaging modalities, including ULM, under anesthesia, such as isoflurane. This anesthetic causes vasodilation, increasing blood vessel size and altering flows[16]. Natural physiology, stress response, and neuronal plasticity are altered with anesthesia, hindering the translation of functional imaging. Consequently, the range of relevant biomarkers that could be faithfully extracted from ULM is reduced. To address this need, we introduce 3D transcranial ULM on habituated, awake mice under stress-free conditions, eliminating the need for anesthesia before imaging[17]. We compare the results of awake ULM to those obtained from the same mice under isoflurane anesthesia.

Moreover, we also report on Open-3DULM, an openly available algorithm for a full 3D ULM reconstruction from beamformed 3D ultrasound data. Previously, an open-source reconstruction algorithm of 2D ULM has been developed and exploited by several laboratories (PALA[18]). To extend in the third dimension and adapt to the new challenges linked to data size, 3D localization, and 3D tracking, we propose a Python algorithmic pipeline accessible to a wide range of users. Additionally, we provide beamformed data from brain acquisitions and results to help the users compare to their home-built 3DULM pipeline. Open-3DULM was also optimized for data processing speed through CPU parallelization.

We performed in-vivo 3D transcranial ULM of the mice brain in awake and anesthetized states (N=5 per group). Supplementary Fig.4a shows the schematic of the experimental setup (the detailed awake protocol can be found in the Methods section). Habituation was performed during four consecutive days before the 3D ULM experiment to ensure a stress-free environment for awake imaging. The mice are first placed in a housing, and a 3D-printed mounting plate was attached to the skull with adhesive, allowing it to be securely fastened into the stereotaxic frame, which ensures no head motion for subsequent imaging. As highlighted in a previous study[19], a 4-day habituation period was enough to ensure that the mice return

to a stress-free state and they are then ready for imaging experiments. Once the head was mounted on the stereotaxic frame, mice first undergo 3D ULM acquisition in an entire awake state for 5 continuous minutes at a volume rate of 250 Hz. This acquisition was followed by another 3D ULM acquisition in an isoflurane-anesthetized state for 5 minutes. The Open-3DULM was applied on 3D ultrasound data that were acquired and beamformed into Brightness mode (B-mode) with a delay and sum algorithm[20], i.e. pixel size of [98.5, 150, 150] micrometers. Beyond the dataset shared with this article (section Code and Data availability), the shared algorithmic pipeline consists of several steps that can be applied to any 3D ultrasound data acquired in-silico, in-vitro, and in-vivo with microbubble injection. First, each volume sequence undergoes filtering to eliminate global tissue motion and skull signals and enhance microbubble signals. Tissue clutter removal was achieved by removing the first 12 among 200 singular vectors using singular value decomposition (SVD) on beamformed 3D data[1,21]. Following the extraction of local maxima, sub-wavelength localization of the microbubbles was performed through radial symmetry algorithm[18]. Finally, the tracking step uses an open-source classical particle tracking algorithm *'simpletracker'*[22] adapted to Open-3DULM. After generating the tracks of individual microbubbles, 3D density i.e. count of mcirobubbles per pixel and mean velocity maps are created for visualization and quantification purposes. These maps enable the measurement of various 3D ULM metrics, which can be used to assess a range of physiological and pathological biomarkers.

Fig.1**a** and **b** show the 3D ULM density rendering of the brain microvasculature in awake (left) and isoflurane (right) states with the same track number and a zoom on the right upper cortex in Fig.1 **c** and **d**. Skeletonization of the vessels was also performed to facilitate the measurements of their diameter. As shown in Fig.1 **e** (awake) and **f** (isoflurane), most vessels in the whole brain are enlarged under anesthesia, as already highlighted in previous studies[16,23]. Finally, 3D ULM velocity maps were also projected on the vessel skeletons. Faster blood velocities were observed in the isoflurane state (Fig.1**h**) compared to awake (Fig.1**g**). Overall, the increase in vessel diameter and blood velocity indicates a an overall elevation in cerebral blood flow (CBF) consistent with previous findings using 2D ULM[17].

For quantification, the vessel area was defined as the number of voxels occupied by a detectable vessel. This metric showed significant differences between the two groups (p-value $\ll 0.01$), i.e. a lower vessel area for awake 3DULM (Fig2**a-c**). Vessel segmentation was achieved thanks to the identification of key vascular structures by two radiologists. Thanks to the Open-3DULM capabilities (Fig.3), selecting a major vessel automatically included all connected branching vessels irrespective of their spatial conformation. Fig.2 highlights various regions of interest (ROIs), including arteries and veins identification. For each ROI, we present the Open-3DULM density map alongside the skeletonized data, detailing the diameter and velocity of each branch. Additionally, two boxplots are generated per vessels region to compare the average branch diameter and velocity between the awake and isoflurane-anesthetized states. The results reveal that all selected veins exhibit significantly reduction in vessel size and velocity in the awake state (purple) compared to under isoflurane (blue) (Region 1, 3 and 5 upward). Interestingly, unlike the 2D ULM study[17], which found no significant changes in arterial measurements, our 3D analysis shows that some arteries also experienced reductions (region 3). Finally, supplementary Fig.5 demonstrates the robustness of our findings, showing consistent results for vessel size (Fig.5**a**) and average velocity (Fig.5**b**) across five different mice.

Overall, experiments on awake habituated animals showed drastic differences in blood flow patterns in the animal brain concerning their anesthetized counterpart. These differences were effectively captured using Open-3DULM, which optimizes quantification in the preclinical setting. The Open-3DULM could become the standard platform to convert any 3D ultrasound acquisition with contrast agents into an in-vivo super-resolution microscope.

Online content

Data Availability

370 blocks of B-mode 3D cineloop for awake state was shared with this publication. Due to the large size of the dataset (2.5 Tb), the remaining data will be shared upon request.

Code Availability

(at publication) All codes are available under the Open-3DULM pipeline presented on GitHub.

References

1. Errico, C. *et al.* Ultrafast ultrasound localization microscopy for deep super-resolution vascular imaging. *Nature* **527**, 499–502 (2015).
2. Christensen-Jeffries, K. *et al.* Super-resolution ultrasound imaging. *Ultrasound medicine & biology* **46**, 865–891 (2020).
3. Couture, O., Hingot, V., Heiles, B., Muleki-Seya, P. & Tanter, M. Ultrasound localization microscopy and super-resolution: A state of the art. *IEEE transactions on ultrasonics, ferroelectrics, frequency control* **65**, 1304–1320 (2018).

4. Song, P., Rubin, J. M. & Lowerison, M. R. Super-resolution ultrasound microvascular imaging: Is it ready for clinical use? *Zeitschrift für Medizinische Physik* (2023).
5. Dencks, S. & Schmitz, G. Ultrasound localization microscopy. *Zeitschrift für Medizinische Physik* (2023).
6. Demené, C. *et al.* Transcranial ultrafast ultrasound localization microscopy of brain vasculature in patients. *Nat. biomedical engineering* **5**, 219–228 (2021).
7. Yan, J. *et al.* Transthoracic ultrasound localization microscopy of myocardial vasculature in patients. *Nat. Biomed. Eng.* 1–12 (2024).
8. Bodard, S. *et al.* Ultrasound localization microscopy of the human kidney allograft on a clinical ultrasound scanner. *Kidney Int.* **103**, 930–935 (2023).
9. Denis, L. *et al.* Sensing ultrasound localization microscopy for the visualization of glomeruli in living rats and humans. *EBioMedicine* **91** (2023).
10. Bodard, S. *et al.* Visualization of renal glomeruli in human native kidneys with sensing ultrasound localization microscopy. *Investig. Radiol.* **59**, 561–568 (2024).
11. Naji, M. A., Taghavi, I., Thomsen, E. V., Larsen, N. B. & Jensen, J. A. Underestimation of flow velocity in 2-d super-resolution ultrasound imaging. *IEEE transactions on ultrasonics, ferroelectrics, frequency control* (2024).
12. Heiles, B. *et al.* Volumetric ultrasound localization microscopy of the whole rat brain microvasculature. *IEEE Open J. Ultrason. Ferroelectr. Freq. Control.* **2**, 261–282 (2022).
13. Chavignon, A. *et al.* 3d transcranial ultrasound localization microscopy in the rat brain with a multiplexed matrix probe. *IEEE Transactions on Biomed. Eng.* **69**, 2132–2142 (2021).
14. Chabouh, G. *et al.* Whole organ volumetric sensing ultrasound localization microscopy for characterization of kidney structure. *IEEE Transactions on Med. Imaging* (2024).
15. Chavignon, A. *et al.* Deep and complex vascular anatomy in the rat brain described with ultrasound localization microscopy in 3d. *IEEE Open J. Ultrason. Ferroelectr. Freq. Control.* **3**, 203–209 (2023).
16. Sullender, C. T., Richards, L. M., He, F., Luan, L. & Dunn, A. K. Dynamics of isoflurane-induced vasodilation and blood flow of cerebral vasculature revealed by multi-exposure speckle imaging. *J. neuroscience methods* **366**, 109434 (2022).
17. Wang, Y. *et al.* Longitudinal awake imaging of deep mouse brain microvasculature with super-resolution ultrasound localization microscopy. *bioRxiv* 2023–09 (2023).
18. Heiles, B. *et al.* Performance benchmarking of microbubble-localization algorithms for ultrasound localization microscopy. *Nat. Biomed. Eng.* **6**, 605–616 (2022).
19. Tsurugizawa, T. *et al.* Awake functional mri detects neural circuit dysfunction in a mouse model of autism. *Sci. advances* **6**, eaav4520 (2020).
20. Perrot, V., Polichetti, M., Varray, F. & Garcia, D. So you think you can das? a viewpoint on delay-and-sum beamforming. *Ultrasonics* **111**, 106309 (2021).
21. Desailly, Y. *et al.* Contrast enhanced ultrasound by real-time spatiotemporal filtering of ultrafast images. *Phys. Medicine & Biol.* **62**, 31 (2016).
22. Tinevez, J.-Y. *et al.* Trackmate: An open and extensible platform for single-particle tracking. *Methods* **115**, 80–90 (2017).
23. Slupe, A. M. & Kirsch, J. R. Effects of anesthesia on cerebral blood flow, metabolism, and neuroprotection. *J. Cereb. Blood Flow & Metab.* **38**, 2192–2208 (2018).
24. Demeulenaere, O. *et al.* Coronary flow assessment using 3-dimensional ultrafast ultrasound localization microscopy. *Cardiovasc. Imaging* **15**, 1193–1208 (2022).

Methods

Animals

All experiments were performed in compliance with the European Community Council Directive of September 22, 2010 (010/63/UE) with ARRIVE guidelines and approved by the protocol APAFIS #35158 validated by the French ethics committee "Comité d'éthique Normandie en matière d'expérimentation animale". Accordingly, the number of animals in our study was kept to the minimum following the 3Rs (reduce, refine, and replace) guidelines. Experiments were performed on N = 5 male (aged 5–7 weeks) Swiss mice (Janvier Labs), weighing 30–40 g at the beginning of the experiments. Animals (housed two per

cage) arrived in the laboratory one week before the start of the experiment. They were maintained under controlled conditions (21 °C, 50-60 % relative humidity, 12/12h light/dark cycle, food and water ad libitum). All animals included in this study were untreated and were used randomly in the various experiments.

Awake protocol condition

Skull cap fixation

Mice were first anesthetized with isoflurane (induction at 5%, maintenance between 1.5% and 2%) in a gas mixture of N2O/O2 (70%/30%) and given buprenorphine (0.1 mg/kg, subcutaneous) for pain relief. The animals were then placed in a stereotaxic frame, keeping their temperature constant at 37°C using a temperature-controlled heating pad. After cleaning and locally anesthetizing the area with Xylocaine (subcutaneous), an incision was made to expose the skull for the attachment of the skull cap (Fig. 4**a**). The skull cap, a 3D-printed PLA structure with an imaging window of 2 cm $\times$ 1.5 cm, was then affixed. The skull surface was treated with hydrogen peroxide and 70% ethanol, followed by a primer which was rinsed with saline. The skull cap was secured in place using dental cement[19].

Habituation

After a 3-day recovery period, a 4-day habituation protocol was implemented to ensure the mice remained still during the ultrasound imaging sessions. Each day, the mice were placed in the housing for progressively longer duration to acclimate them to the restraint conditions. We selected a 4-day habituation period based on prior research involving functional magnetic resonance imaging (fMRI) in mice[19]. In this study, they demonstrated that after 4 days, mice exhibited normalized heart rates, respiratory rates, and corticosterone levels, indicating a return to a stress-free state.

Catheter placement

To avoid the effects of isoflurane anesthesia on ultrasound imaging, the catheter was placed a day in advance. The day before ultrasound imaging, the mice were anesthetized with isoflurane (5% induction, 1.5%-2% maintenance) in a gas mixture of N2O/O2 (70%/30%). They were given buprenorphine (0.05 mg/kg, subcutaneous) for pain relief and then positioned in a stereotaxic frame within their housing. A regulated heating pad kept their body temperature stable at 37°C. A catheter was then inserted into the tail vein and secured with adhesive tape to enable intravenous (IV) injections of microbubbles.

Preparation for imaging

The animals were secured in a small animal stereotaxic frame (David Kopf stereotaxic instrument, Tujunga, CA, USA). Imaging was first performed on awake animals, followed by applying an anesthesia mask delivering a mixture of isoflurane (2%) and nitrous oxide. Heart and respiratory rates were continuously monitored to maintain stable anesthesia (Labchart, AD Instruments). Two milliliters of saline were gently applied to the brain, preserving the dura mater's integrity, and followed by ultrasound gel (Neo Jelly US, France). The ultrasonic probe was then precisely positioned using the stereotaxic electrode manipulator (0.1 mm resolution, David Kopf stereotaxic instrument) fitted with a custom 3D-printed probe holder.

Microbubble contrast agent injections

During the 5-minute imaging period, 25 μL of SonoVue microbubbles, prepared using the standardized clinical protocol, were injected into the tail vein catheter every minute, resulting in a total volume of 150 µL. To prevent the microbubbles from floating to the top of the syringe, gentle agitation was achieved using two magnets, one placed inside the syringe and one outside. If the microbubbles solution became clear, the syringe was replaced at least once during the imaging session.

3D ultrasound imaging

Ultrasound data was acquired using a single Verasonics 256-channel research scanner (Kirkland, USA) coupled with a 1024-elements matrix probe from Vermon (Tours, France) with a central frequency of 7.8 MHz and 56% bandwidth at -6 dB. The probe connected to the Vantage 256 system through a Verasonics UTA 1024-MUX adapter. The imaging protocol employed an ultrafast sequence of five plane waves, oriented at $\pm 5^{\circ}$ in both elevation and lateral directions, with a maximum pulse repetition frequency (PRF) of 16 kHz. Each pulse was a 2-cycle emission at 67% duty cycle, driven at 10 volts, producing a Peak Negative Pressure (PNP) of 298 kPa and a mechanical index (MI) of 0.1. The probe was divided into four 256-element panels, and during transmission, each panel received signals from its neighboring panels, requiring ten emissions per angle[13]. Five hundred sequences, each containing two hundred continuous volumes at 250 Hz, were recorded over approximately four minutes, resulting in about 250 GB of data. Each block required approximately 0.5 seconds to be saved continuously. The acquired volumes were sampled with a 50% bandwidth.

3D beamforming

The data were then reconstructed with a classical delay and sum beamforming[20] on a [98.5, 150, 150] μm grid, before reaching the final 3D ULM resolution of [9.85, 9.85,9.85] μm.

Statistical analysis

Statistical analyses were conducted to compare brain regions between awake and isoflurane-anesthetized states, utilizing a non-parametric Mann-Whitney test in GraphPad Prism 9 software. The significance levels of the findings are reported as follows: $ns = P \geq 0.05$, $\star = P \leq 0.05$, $\star\star = P \leq 0.01$, $\star\star\star = P \leq 0.001$, $\star\star\star\star = P \leq 0.0001$.

Open 3DULM: Algorithm

Clutter filter

After obtaining a 3D ultrasound data and beamformed into Brightness mode (B-mode) volumes, the first step of the Open 3DULM algorithm is to remove the tissue signal, tissue motion as well as the skull signal to enhance microbubbles signal. Clutter filtering was performed using the Singular Value Decomposition (SVD) technique[1,21]. The user could specify the number of singular vectors to remove. In this study, we removed 12 out of 200. This threshold was empirically determined and applied uniformly across all animals.

Localization

The second step in the Open-3DULM algorithm was the localization of the Point Spread Function (PSF) of the microbubbles. We specified the number of microbubbles (*'number_of_particles'*) present in one volume at a specific frame. In this work, we set this parameter to 900. The 3D full-width-half-maximum (*'fwhm'*) of the PSF for the microbubbles was defined as *fwhm* = $[5 \times 5 \times 5]$ as data was beamformed at half of a wavelength in all directions. We used *fwhm* = $[5 \times 5 \times 5]$. After selecting the number of microbubbles per frame and the PSF size, the algorithm localized the regional maxima of the filtered data (3D+time) by applying the *'maximumFilter'* function from *'scipy.ndimage'*, arranging the pixels from the highest intensity value to the lowest. To ensure that the high-intensity pixels were likely to be microbubbles, the algorithm computed the local Signal-to-Noise Ratio (SNR) within a user-defined patch size *('patch_size')*. In this work, the patch size was set to $[7 \times 7 \times 7]$ to consider an area larger than the microbubble spot (fwhm). We also specified the minimum SNR *('min_snr')* for an accepted microbubble PSF and the number of local maxima within the chosen patch (*'nb_local_max'*). The algorithm selects the (*'number_of_particles'*) meeting the minimum SNR and (*'nb_local_max'*) conditions, starting with the localized microbubbles with the highest SNR.

Sub-wavelength localization

For each localized PSF within the patches, 3D radial symmetry[12] was employed to pinpoint the microbubble's position with sub-wavelength precision. A *'localization'* matrix was then generated, containing five columns: the local SNR of the microbubble, the z, x, and y positions, and the frame number.

3D tracking

Once the subwavelength localization step was completed, the *'localization'* matrix was sent to the 3D tracking final step in the Open-3DULM algorithm. The 3D tracking algorithm is a library Python-adapted (*'PeasyTracker'*) version of the open-source '*SimpleTracker*'[22]. It uses the Hungarian algorithm to minimize the Euclidean distance between points in consecutive frames. Table 1 summarizes the localization and tracking parameters, their explanations, and the values used in this work. The interpolation step was done using the *'interp'* function from the *Numpy* library with an interpolation factor of 1 over the resolution factor *'res'* that should be defined by the user. Here, we used a factor of 10 (*res* = 10). Finally, the *'tracks'* structure was then computed with all the tracks, i.e. the raw and the interpolated ones.

Open 3DULM: Image analysis

Once the tracks are generated, they were used to create a 3DULM density rendering (*output_density*), which was a 3D matrix where each voxel's value represents the number of times a track passed through that voxel. Additionally, the tracks were used to create 3DULM velocity maps, including the norm of the 3D velocity (*output_velocity*) and the velocity with directionality (*output_directivity*), indicating upward and downward velocity direction in the axial z direction. Open-3DULM rendering were computed by loading the *output_density* into Amira (Amira 2019 software, FEI) and using the Volume Rendering function for 3DULM density rendering. To skeletonize the vasculature[24], a Gaussian filter ($\sigma = [1,1,1]$ px) was first applied, followed by the 'auto-skeleton' function in Amira (Figure 2**e** and **f**). For 3D velocity rendering, *output_velocity* was loaded into Amira and used as a colormap on the skeletonized structure (Figure 2**g** and **h**).

Acknowledgements

We thank Oscar Demeulenaere for his help regarding skeletenization on AMIRA software.

Table 1. Open-3DULM: 3D localization and tracking parameters to be defined by the user

Open-3DULM parameters	Explanation	Values adopted in this work
SVD filtering ([min_svd_value max_svd_value])	The range of accepted singular values	12-200
Bandpass filter ([left_cutoff_bandpass right_cutoff_bandpass]) and the order (filter_order)	The lower and upper-frequency bounds	not applied in this work
Full-width-half-maximum (fwhm)	The size of the PSF of the microbubbles	$[3 \times 3 \times 3]$
Patch size (patch_size)	The size of the 3D kernel where the local SNR is computed	$[7 \times 7 \times 7]$
Minimum SNR (min_snr)	The minimum SNR value for a microbubble to be accepted	9
Number of local maxima in the patch nb_local_max	The maximum number of allowed microbubbles inside a patch	10
Number of particles (number_of_particles)	The number of microbubbles to be localized in every frame	900
Maximum Velocity (mm/s) (max_velocity)	Maximum velocity in mm/s, which is converted into the maximum linking distance, i.e., the maximum allowed distance travelled by a particle between two frames	30 mm/s
Max Gap Closing (max_gap_closing)	The maximum number of frames that the microbubble is allowed to disappear and reappear	0
Minimum Length (min_length)	The minimum number of frames a microbubble must be tracked for it to be accepted	9
Resolution factor (res)	The hypothetical super-resolution factor	10

Author contributions

G.C. M.A. D.V. C.O. O.C. designed the research. G.C. L.D. M.A. did the experiments. G.C. L.D. A.C. B.H. developed the acquisition sequence, ULM reconstruction, and analysis framework. G.C. L.D. B.P. S.B. O.C. analyzed the processed data. JB.D. J.B. G.C. L.D. made the code available on Gitlab. G.C. L.D. made the data available on the ZENODO platform. All the authors discussed the results and wrote the paper.

Competing interests

O.C. is the holder of patents concerning super-resolution ultrasound imaging. He is also a co-founder and share-holder in the startup ResolveStroke.

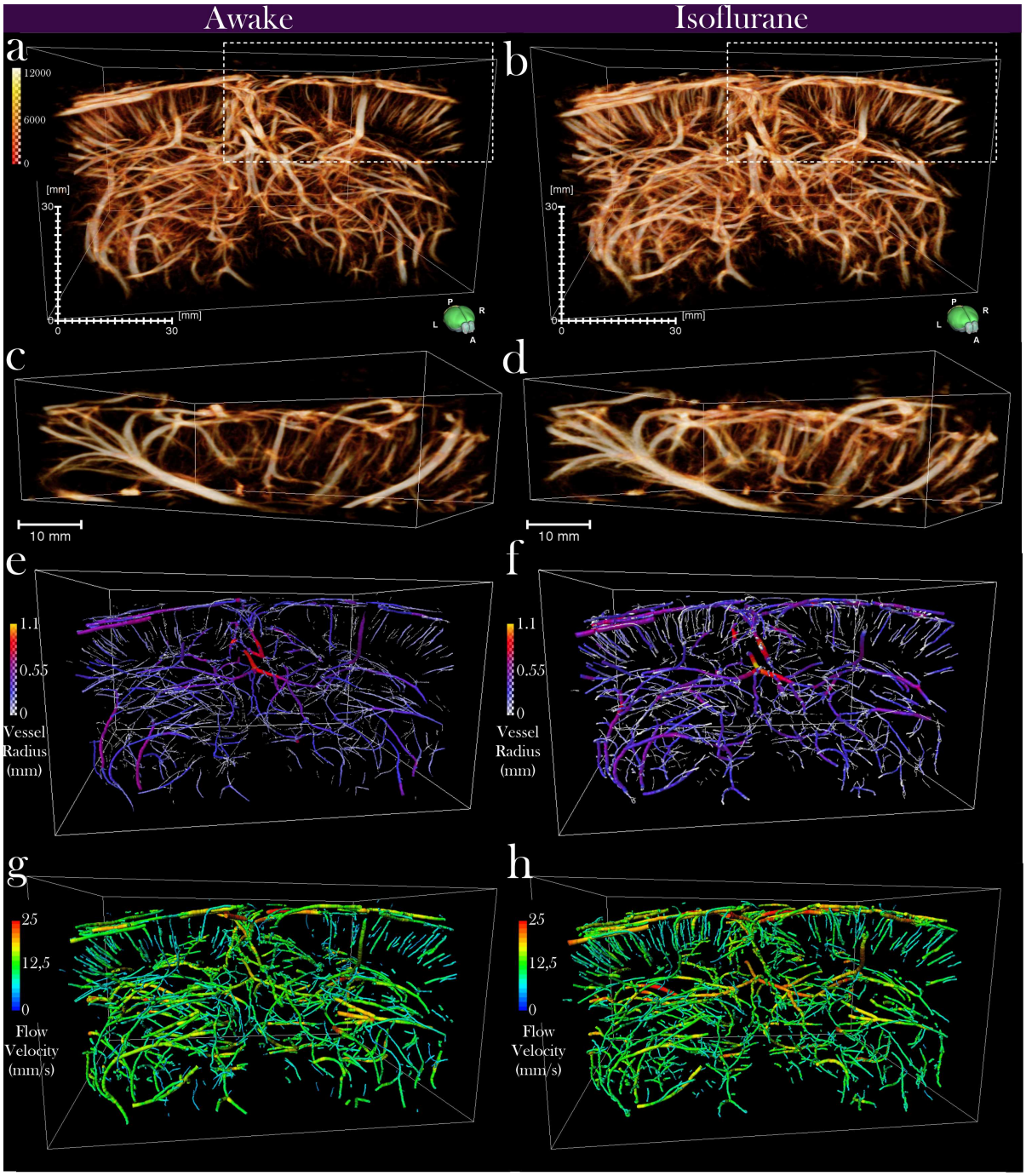

Figure 1. 3D transcranial Ultrasound Localization Microscopy in awake (left) and isoflurane-anesthetized (right) mice. **a**,**b** 3DULM density map, with a zoom on the cortical area **c** and **d**. Vessel diameter quantification **e** and **f** after skeletonization. 3DULM Velocity maps quantification **g** and **h**.

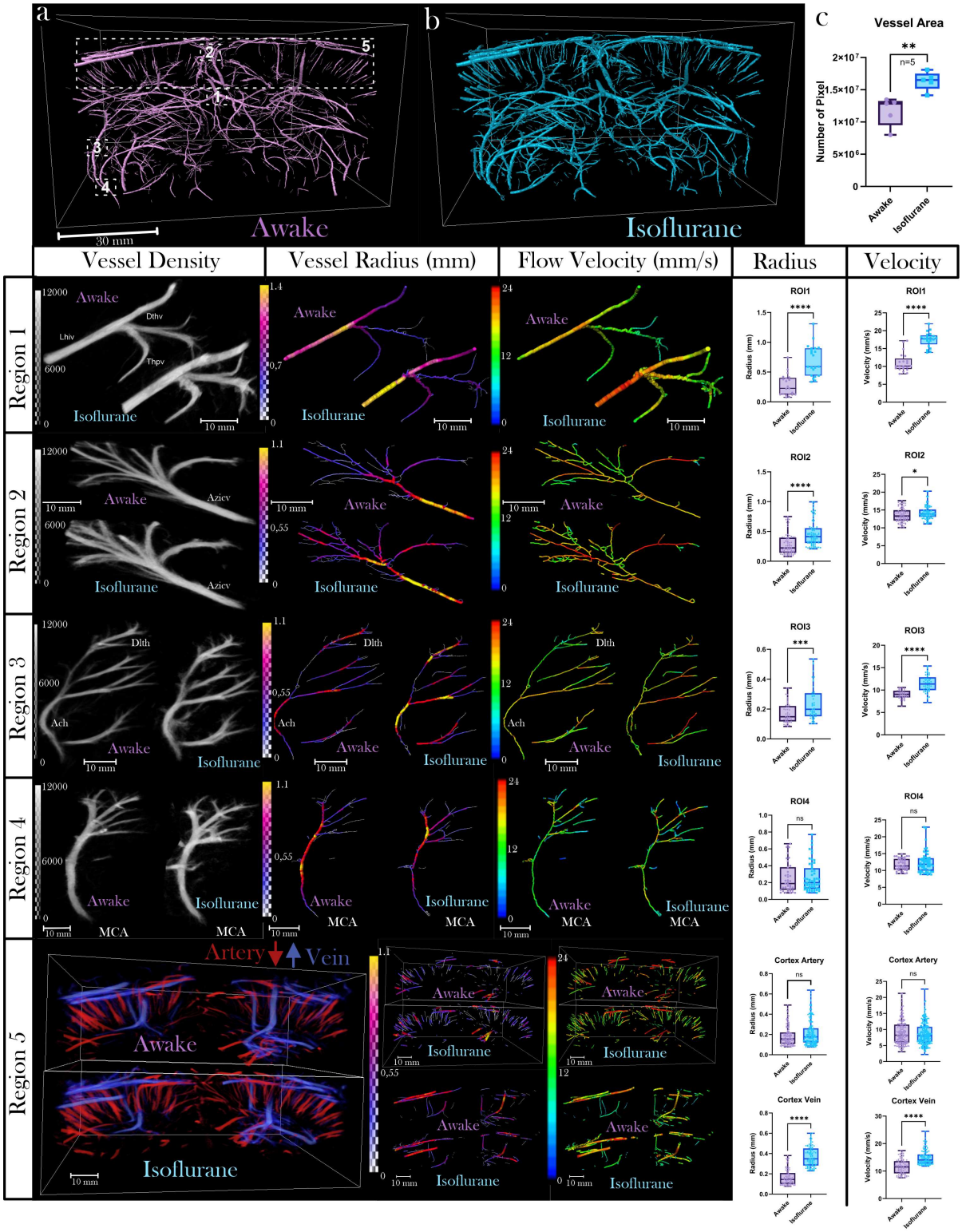

Figure 2. Comparative analysis on a wide range of vesselsa, **b**: vessel diameter maps with definition of the different regions. **c**: Boxplot of vessel area metric showing greater vessel occupancy in isoflurane state. Five regions of interest include the cortex with arteries (red, downward flow) and veins (blue, upward flow). For each ROI, 3D ULM density maps, vessel diameters, and velocities are displayed. Boxplots for each ROI depict the average radius and velocity of branches, comparing awake (purple) and isoflurane (cyan) states. Lhiv (longitudinal hippocampal vein); Dthv (dorsal thalamus vein); Thpv (thalamoperforating vein); Ach (anterior choroidal artery); Dlth (dorsolateral hypothalamus); MCA (middle cerebral artery)

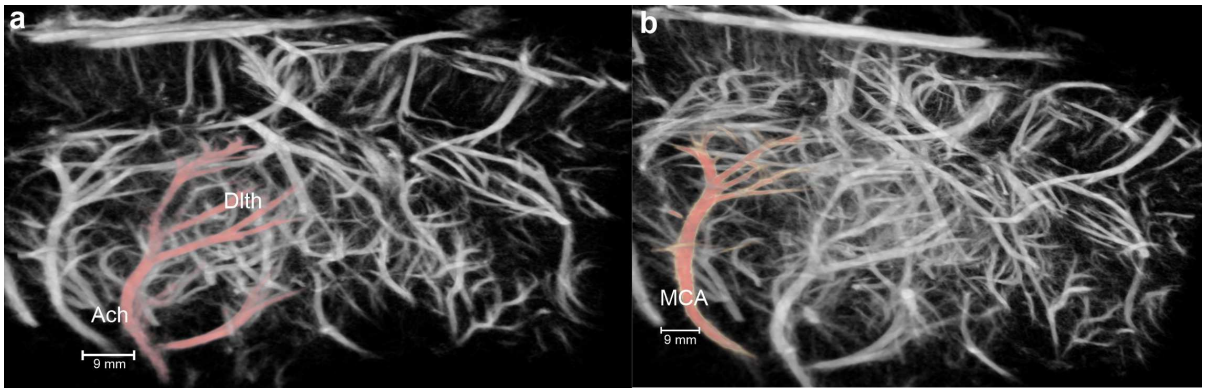

Figure 3. 3D automatic segmentation of vasculature using Open-3DULM and AMIRA (Amira 2019 software, FEI): The watershed-like 3D vascular structure of Open-3DULM enables automatic segmentation of vessels, identifying the connections between branches and the main vessel. **a** Region 3 (Ach: anterior choroidal artery); Dlth (dorsolateral hypothalamus) and **b** Region 4 (MCA: middle cerebral artery).

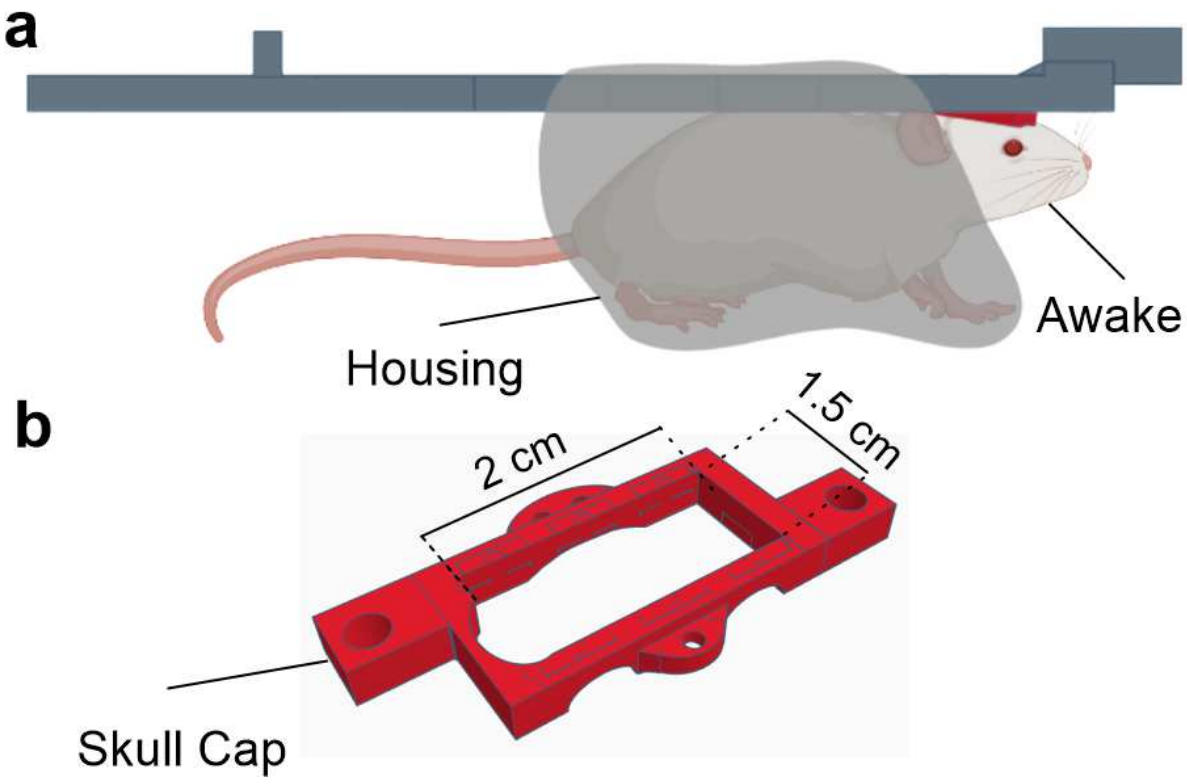

Figure 4. Setup for awake mice ultrasound imaging: a 3D printed structure and housing for habituated awake mice, and **b** 3D printed PLA skull cap for secure attachment to the stereotaxic frame during ultrasound imaging.

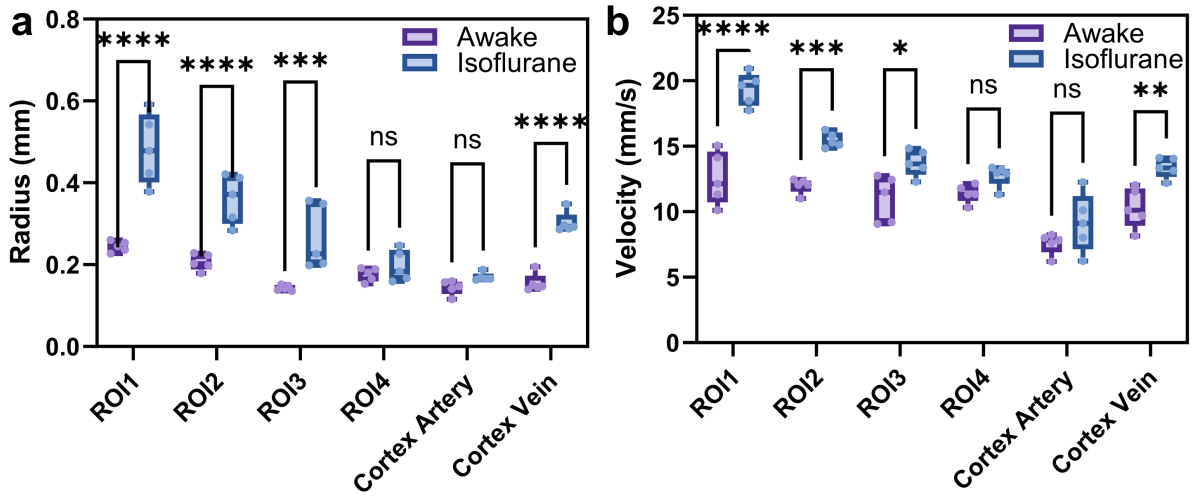

Figure 5. General quantification differentiates the awake from the anaesthetized (isoflurane) groups: Average ROI **a** radius measurement and **b** average velocity measurement in awake versus isoflurane-anesthetized mice (N=5 mice per group)